

# Hidden magnetic transitions in thermoelectric layered cobaltite, $[\text{Ca}_2\text{CoO}_3]_{0.62}[\text{CoO}_2]$

J. Sugiyama<sup>1,\*</sup>, J. H. Brewer<sup>2</sup>, E. J. Ansaldo<sup>3</sup>, H. Itahara<sup>1</sup>, K. Dohmae<sup>1</sup>, Y. Seno<sup>1</sup>, C. Xia<sup>1</sup>, and T. Tani<sup>1</sup>

<sup>1</sup>*Toyota Central Research and Development Labs. Inc., Nagakute, Aichi 480-1192, Japan*

<sup>2</sup>*TRIUMF, CIAR and Department of Physics and Astronomy,  
University of British Columbia, Vancouver, BC, V6T 1Z1 Canada and*

<sup>3</sup>*Department of Physics, University of Saskatchewan, Saskatoon, SK, S7N 5A5 Canada*

(Dated: August 27, 2018)

A positive muon spin rotation and relaxation ( $\mu^+$ SR) experiment on  $[\text{Ca}_2\text{CoO}_3]_{0.62}[\text{CoO}_2]$ , (*i.e.*,  $\text{Ca}_3\text{Co}_4\text{O}_9$ , a layered thermoelectric cobaltite) indicates the existence of two magnetic transitions at  $\sim 100$  K and 400 - 600 K; the former is a transition from a paramagnetic state to an incommensurate (IC) spin density wave (SDW) state. The anisotropic behavior of zero-field  $\mu^+$ SR spectra at 5 K suggests that the IC-SDW propagates in the  $a$ - $b$  plane, with oscillating moments directed along the  $c$ -axis; also the IC-SDW is found to exist not in the  $[\text{Ca}_2\text{CoO}_3]$  subsystem but in the  $[\text{CoO}_2]$  subsystem. In addition, it is found that the long-range IC-SDW order completes below  $\sim 30$  K, whereas the short-range order appears below 100 K. The latter transition is interpreted as a gradual change in the spin state of Co ions above 400 K. These two magnetic transitions detected by  $\mu^+$ SR are found to correlate closely with the transport properties of  $[\text{Ca}_2\text{CoO}_3]_{0.62}[\text{CoO}_2]$ .

PACS numbers: 76.75.+i, 75.30.Fv, 75.50.Gg, 72.15.Jf

Keywords: thermoelectric layered cobaltites, magnetism, muon spin rotation, incommensurate spin density waves, spin state transition

## I. INTRODUCTION

A strong correlation between  $3d$  electrons induces important physical properties in  $3d$  metal oxides; *e.g.* high temperature superconductivity in cuprates, colossal magnetoresistance in manganites and probably 'good' thermoelectric properties in layered cobaltites. Four cobaltites,  $[\text{Ca}_2\text{CoO}_3]_{0.62}[\text{CoO}_2]$ , [1, 2, 3]  $\text{Na}_x\text{CoO}_2$  with  $x \sim 0.6$ , [4, 5, 6]  $[\text{Sr}_2\text{Bi}_{2-y}\text{Pb}_y\text{O}_4]_x[\text{CoO}_2]$ , [7, 8, 9] and  $[\text{Ca}_2\text{Co}_{4/3}\text{Cu}_{2/3}\text{O}_4]_{0.62}[\text{CoO}_2]$ , [10] are known to be good thermoelectrics because of their metallic conductivities and high thermoelectric powers, for reasons which are currently not fully understood. In order to find excellent thermoelectrics suitable for thermoelectric power generation for protecting the environment by saving energy resources and reducing the release of  $\text{CO}_2$  into the atmosphere, it is crucial to understand the mechanism of the 'good' thermoelectric properties in these layered cobaltites.

The layered cobaltites share a common structural component: the  $\text{CoO}_2$  planes, in which a two-dimensional-triangular lattice of Co ions is formed by a network of edge-sharing  $\text{CoO}_6$  octahedra. Charge carrier transport in these materials is thought to be restricted mainly to these  $\text{CoO}_2$  planes, as in the case of the  $\text{CuO}_2$  planes for the high- $T_c$  cuprates. Since specific heat measurements on  $\text{Na}_x\text{CoO}_2$  indicate a large thermal effective mass of carriers [11], all these cobaltites are believed to be strongly correlated electron systems.

The crystal structure of  $[\text{Ca}_2\text{CoO}_3]_{0.62}[\text{CoO}_2]$  consists of alternating layers of the triple rocksalt-type  $[\text{Ca}_2\text{CoO}_3]$  subsystem and the single  $\text{CdI}_2$ -type  $[\text{CoO}_2]$  subsystem stacked along the  $c$ -axis [2, 3, 12]. There is a misfit between these subsystems along the  $b$ -axis. Susceptibility ( $\chi$ ) measurements [2, 13] indicate two magnetic transitions at 19 K and 380 K; the former is a ferrimagnetic transition ( $T_{\text{FR}}$ ) and the latter is probably a spin-state transition ( $T_{\text{SS}}^X$ ). The temperature dependence of the resistivity  $\rho$  exhibits a broad minimum around 80 K [2, 3, 13] and a broad maximum between 400 and 600 K [2]. Although  $\rho$  appears to diverge with decreasing temperature below  $T_{\text{FR}}$ , it is worth noting that  $\chi(T)$  shows no clear anomalies near 80 K or 600 K.

A recent positive muon spin rotation and relaxation ( $\mu^+$ SR) experiment [13, 14] indicated the existence of an incommensurate (IC) spin density wave (SDW) state below 100 K, which was not detected previously by other magnetic measurements [2, 3]. Thus, the broad minimum around 80 K in the  $\rho(T)$  curve suggests that the behavior of conduction electrons is strongly affected by the IC-SDW order in  $[\text{Ca}_2\text{CoO}_3]_{0.62}[\text{CoO}_2]$ . Nevertheless, we need more information to confirm the correlation between the transport properties and the IC-SDW in  $[\text{Ca}_2\text{CoO}_3]_{0.62}[\text{CoO}_2]$ ; such as the structure of the IC-SDW and the subsystem in which the IC-SDW exists. Furthermore,  $T_{\text{SS}}^X$  ( $\sim 380$  K) is too low to explain the whole change in the  $\rho(T)$  curve between 400 and 600 K, while the  $\mu^+$ SR experiment showed a change in slope of the relaxation rate-vs.- $T$  curve above 400 K.[14]

In order to further clarify the role of magnetism in thermoelectric layered cobaltites, we have measured both weak ( $\sim 100$  Oe) transverse-field positive muon spin rotation and relaxation (wTF- $\mu^+$ SR) and zero field (ZF-)

\*Electronic address: sugiyama@iclub.tytlabs.co.jp

$\mu^+$ SR time spectra in  $[\text{Ca}_2\text{CoO}_3]_{0.62}[\text{CoO}_2]$  at temperatures below 700 K. The former method is sensitive to local magnetic order *via* the shift of the  $\mu^+$  spin precession frequency and the enhanced  $\mu^+$  spin relaxation, while ZF- $\mu^+$ SR is sensitive to weak local magnetic [dis]order in samples exhibiting quasi-static paramagnetic moments.

## II. EXPERIMENT

A randomly oriented polycrystalline disk ( $\sim 20$  mm diameter and  $\sim 2$  mm thick) of  $[\text{Ca}_2\text{CoO}_3]_{0.62}[\text{CoO}_2]$  was synthesized by a conventional solid state reaction technique [13]. *C*-axis aligned polycrystalline  $[\text{Ca}_2\text{CoO}_3]_{0.62}[\text{CoO}_2]$  and  $[\text{Ca}_{1.8}M_{0.2}\text{CoO}_3]_{0.62}[\text{CoO}_2]$  ( $M = \text{Sr}, \text{Y}, \text{Bi}$ ) plates ( $\sim 20 \times 20 \times 2$  mm<sup>3</sup>) were synthesized by a reactive templated grain growth technique [15]. Single-crystal platelets of  $[\text{Ca}_2\text{CoO}_3]_{0.62}[\text{CoO}_2]$  ( $\sim 5 \times 5 \times 0.1$  mm<sup>3</sup>) were prepared by a  $\text{SrCl}_2$  flux method [16]. Then, all the samples were annealed in an  $\text{O}_2$  flow at 450 °C for 12 hours. The preparation and characterization of these samples were described in detail elsewhere [17, 18]. The  $\mu$ SR experiments were performed on the **M20** and **M15** surface muon beam line at TRIUMF. The experimental setup is described elsewhere [19].

## III. RESULTS

### A. IC-SDW transition

In all the  $[\text{Ca}_2\text{CoO}_3]_{0.62}[\text{CoO}_2]$  samples, the wTF- $\mu^+$ SR spectra in a magnetic field of  $H \sim 100$  Oe exhibit a clear reduction of the  $\mu^+$  precession amplitude below 100 K. The data were obtained by fitting the wTF- $\mu^+$ SR spectrum in the time domain with a combination of a slowly relaxing precessing signal and two non-oscillatory signals, one fast and the other slow relaxing:

$$A_0 P(t) = A_{\text{PARA}} \exp(-\lambda_{\text{PARA}} t) \cos(\omega_{\mu} t + \phi) + A_{\text{fast}} \exp(-\lambda_{\text{fast}} t) + A_{\text{slow}} \exp(-\lambda_{\text{slow}} t), \quad (1)$$

where  $A_0$  is the initial asymmetry,  $P(t)$  is the muon spin polarization function,  $\omega_{\mu}$  is the muon Larmor frequency,  $\phi$  is the initial phase of the precession and  $A_n$  and  $\lambda_n$  ( $n = \text{PARA}, \text{fast}$  and  $\text{slow}$ ) are the asymmetries and exponential relaxation rates of the three signals. The latter two signals ( $n = \text{fast}$  and  $\text{slow}$ ) have finite amplitudes below  $T_{\text{SDW}}^{\text{on}} \approx 100$  K and probably suggest the existence of multiple muon sites in  $[\text{Ca}_2\text{CoO}_3]_{0.62}[\text{CoO}_2]$ .

Figures 1(a) and 1(b) show the temperature dependences of the paramagnetic asymmetry  $A_{\text{PARA}}$  (which is proportional to the volume fraction of a paramagnetic phase in the sample) and the corresponding relaxation

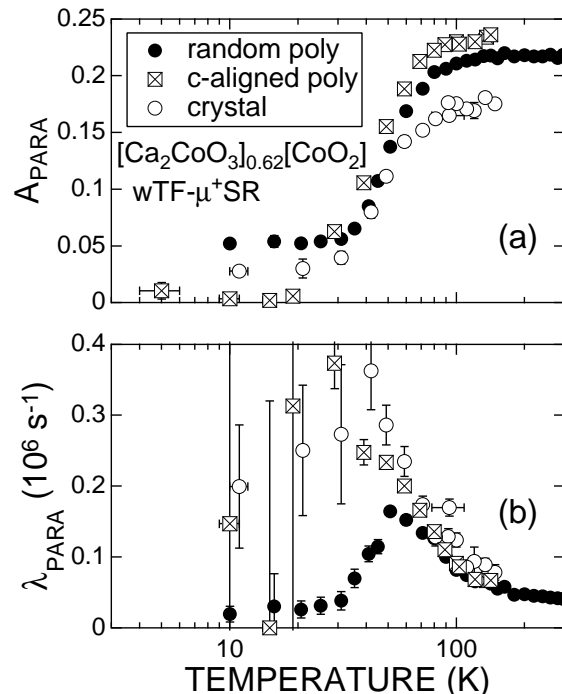


FIG. 1: (a) Paramagnetic  $\mu^+$  spin precession asymmetry  $A_{\text{PARA}}$  and (b) muon spin relaxation rate  $\lambda_{\text{PARA}}$  as a function of temperature for the three  $[\text{Ca}_2\text{CoO}_3]_{0.62}[\text{CoO}_2]$  samples: a randomly oriented polycrystalline disk (solid circles) [13], a *c*-axis aligned polycrystalline plate (squares) and single crystal (sc) platelets (open circles). For the sc platelets, both the value of  $A_{\text{PARA}}$  above 100 K and the change in  $A_{\text{PARA}}$  below 100 K are smaller than those in the polycrystalline samples. This is because the muon momentum was decreased from 28 to 25 MeV/c for the sc measurements to stop muons in the thin platelets ( $\sim 100$   $\mu\text{m}$  thickness), causing a small background signal from muons stopping elsewhere.

rate  $\lambda_{\text{PARA}}$  in three  $[\text{Ca}_2\text{CoO}_3]_{0.62}[\text{CoO}_2]$  samples: a randomly oriented polycrystalline sample [13], a *c*-aligned polycrystalline sample, and single crystal platelets. The large decrease in  $A_{\text{PARA}}$  below 100 K (and the accompanying increase in  $\lambda_{\text{PARA}}$ ) indicate the existence of a magnetic transition with an onset temperature  $T_c^{\text{on}} \approx 100$  K and a transition width  $\Delta T \approx 70$  K. The single crystal data suggest that the large  $\Delta T$  is not caused by inhomogeneity of the sample but is an intrinsic property of this compound.

Figure 2 shows ZF- $\mu^+$ SR time spectra at 4.8 K in the *c*-aligned sample; the top spectrum was obtained with the initial  $\mu^+$  spin direction  $\vec{S}_{\mu}(0)$  perpendicular to the *c*-axis and the bottom one with  $\vec{S}_{\mu}(0) \parallel \hat{c}$ . A clear oscillation due to quasi-static internal fields is observed only when  $\vec{S}_{\mu}(0) \perp \hat{c}$ . The time interval from  $t = 0$  to the first zero crossing of that oscillation is roughly the same (1 : 1.2954) as the interval between the first and second zero crossings; this is a characteristic of a zeroth-order Bessel

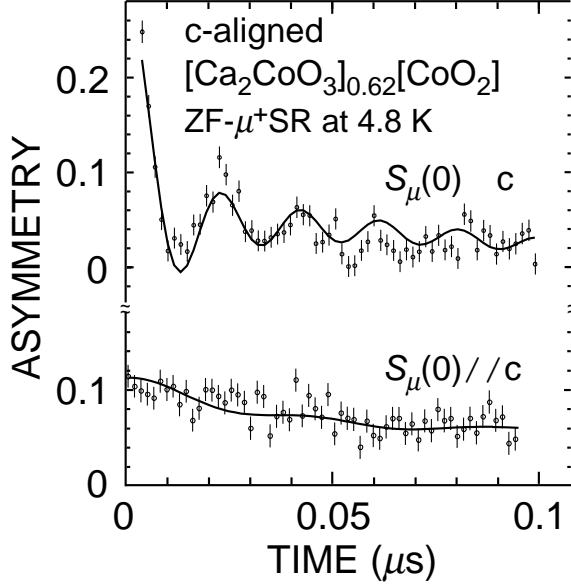


FIG. 2: ZF- $\mu^+$ SR time spectra of the  $c$ -aligned  $[\text{Ca}_2\text{CoO}_3]_{0.62}[\text{CoO}_2]$  plate at 4.8 K. The configurations of the sample and the initial muon spin direction  $\vec{S}_\mu(0)$  are (top)  $\vec{S}_\mu(0) \perp \hat{c}$  and (bottom)  $\vec{S}_\mu(0) \parallel \hat{c}$ .

function of the first kind  $J_0(\omega_\mu t)$  that describes the muon polarization evolution in an incommensurate spin density wave IC-SDW field distribution [19, 20, 21].

Actually, the top oscillating spectrum was fitted using a combination of three signals:

$$A_0 P(t) = A_{\text{SDW}} J_0(\omega_\mu t) \exp(-\lambda_{\text{SDW}} t) + A_{\text{KT}} G_{zz}^{\text{KT}}(t, \Delta) + A_{\text{tail}} \exp(-\lambda_{\text{tail}} t), \quad (2)$$

$$\omega_\mu \equiv 2\pi\nu_\mu = \gamma_\mu H_{\text{int}}, \quad (3)$$

$$G_{zz}^{\text{KT}}(t, \Delta) = \frac{1}{3} + \frac{2}{3} (1 - \Delta^2 t^2) \exp(-\Delta^2 t^2 / 2), \quad (4)$$

where  $A_0$  is the empirical maximum muon decay asymmetry,  $A_{\text{SDW}}$ ,  $A_{\text{KT}}$  and  $A_{\text{tail}}$  are the asymmetries associated with the three signals,  $G_{zz}^{\text{KT}}(t, \Delta)$  is the static Gaussian Kubo-Toyabe function,  $\Delta$  is the static width of the distribution of local frequencies at the disordered sites and  $\lambda_{\text{tail}}$  is the slow relaxation rate of the 'tail' (not shown in this Figure), and the fit using an exponential relaxed cosine oscillation,  $\exp(-\lambda t) \cos(\omega_\mu t + \phi)$ , provides a phase angle  $\phi \sim 90^\circ$ , which is physically meaningless.[22]

We therefore conclude that  $[\text{Ca}_2\text{CoO}_3]_{0.62}[\text{CoO}_2]$  undergoes a magnetic transition from a paramagnetic state to an IC-SDW state (*i.e.*  $T_c^{\text{on}} = T_{\text{SDW}}^{\text{on}}$ ). The absence of

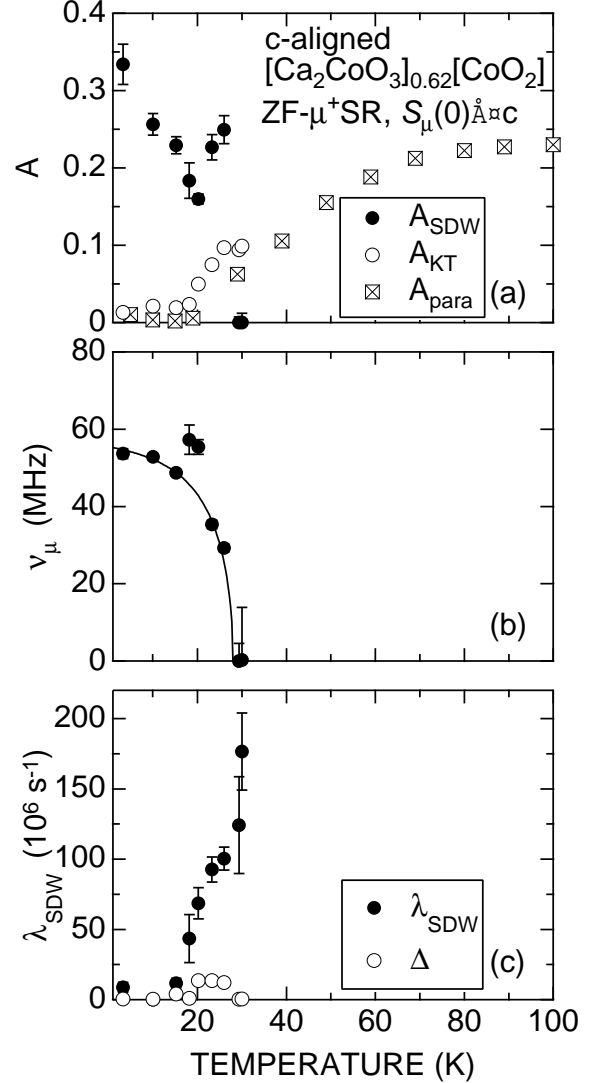


FIG. 3: Temperature dependences of (a)  $A_{\text{SDW}}$  and  $A_{\text{PARA}}$  (estimated by the wTF- $\mu^+$ SR experiment), (b)  $\nu_\mu$  and (c)  $\lambda_{\text{SDW}}$  for the  $c$ -aligned  $[\text{Ca}_2\text{CoO}_3]_{0.62}[\text{CoO}_2]$ . The solid line in Fig. 3(b) represents the temperature dependence of the BCS gap energy. The deviation of the experimental data from the theory around 20 K is probably due to the effect of the ferrimagnetic transition at 19 K.

a clear oscillation in the bottom spectrum of Fig. 2 indicates that the internal magnetic field  $\vec{H}_{\text{int}}$  is roughly parallel to the  $c$ -axis, since the muon spins do not precess in a parallel magnetic field. The IC-SDW is unlikely to propagate along the  $c$ -axis due both to the two-dimensionality and to the misfit between the two subsystems. The IC-SDW is therefore considered to propagate in the  $a$ - $b$  plane, with oscillating moments directed along the  $c$ -axis. This suggests that the ferrimagnetic interaction is also parallel to the  $c$ -axis, and is consistent with the results of our  $\chi$  measurement on single crystals.[23]

Figures 3(a)-3(c) show the temperature dependences of  $A_{\text{SDW}}$ ,  $A_{\text{KT}}$  and  $A_{\text{PARA}}$  (same in Fig. 1),  $\nu_{\mu}$  and  $\lambda_{\text{SDW}}$  and  $\Delta$  for the  $c$ -aligned  $[\text{Ca}_2\text{CoO}_3]_{0.62}^{\text{RS}}[\text{CoO}_2]$ .  $A_{\text{SDW}}$  increases with decreasing  $T$  below 30 K, although  $A_{\text{PARA}}$  obtained by the wTF- $\mu^+$ SR measurement exhibits a rapid decrease below 100 K and levels off to almost 0 below 30 K (see Fig. 3(a)). According to the recent  $\chi$  measurements using single crystal platelets,[23] a small shoulder in the  $\chi(T)$  curve was observed at 27 K only for  $H \perp ab$ . This temperature (27 K) corresponds to the highest temperature that a clear  $\mu^+$ SR signal due to the IC-SDW was observed. Thus, it is considered that a short-range order IC-SDW state appears below 100 K =  $T_{\text{SDW}}^{\text{on}}$ , while the long-range order is completed below 27 K; *i.e.*,  $T_{\text{SDW}} = T_{\text{SDW}}^{\text{end}}$ . Since both  $\rho(T)$  and  $S(T)$  are metallic above 80 K and semiconducting below 80 K,[2, 3] charge carrier transport is strongly affected by a formation of the short-range IC-SDW order.

Although the  $\nu_{\mu}(T)$  curve is well explained by the BCS weak coupling theory as expected for the IC-SDW state,[24] there is a deviation from the theory around 20 K (see Fig. 3(b)). This deviation (and the accompanying increase in  $A_{\text{SDW}}$ ) is probably due to the effect of the ferrimagnetic transition at 19 K (=  $T_{\text{FR}}$ ). Here, the ferrimagnetism is considered to be caused by an interlayer coupling between Co spins in the  $[\text{Ca}_2\text{CoO}_3]$  and  $[\text{CoO}_2]$  subsystems,[23] while the IC-SDW order completes below 27 K. This means that the IC-SDW is affected by the ferrimagnetic coupling *via*. the Co spins in the  $[\text{Ca}_2\text{CoO}_3]$  subsystem. Therefore, the enhancement of the internal magnetic field at  $T_{\text{FR}}$  is likely to be caused by a critical phenomenon around the ferrimagnetic transition. In addition, the magnitude of  $\lambda_{\text{SDW}}$  decreases rapidly with decreasing  $T$  and levels off to a constant value below 20 K. This suggests that the broadening of the IC-SDW field distribution at the  $\mu^+$  sites mainly occurs in the temperature range between  $T_{\text{SDW}}$  and  $T_{\text{FR}}$ .

In order to determine the subsystem in which the IC-SDW exists, ZF- $\mu^+$ SR spectra were measured in doped samples:  $c$ -aligned polycrystalline  $[\text{Ca}_{1.8}M_{0.2}\text{CoO}_3]_{0.62}[\text{CoO}_2]$  ( $M = \text{Sr}, \text{Y}$  and  $\text{Bi}$ ). A clear precession was observed in the ZF- $\mu^+$ SR spectrum with  $\vec{S}_{\mu}(0) \perp \hat{c}$  in every sample, although  $T_{\text{SDW}}$  depended on dopant. Figure 4 shows the temperature dependences of  $\nu_{\mu}$  for the  $c$ -aligned pure and doped  $[\text{Ca}_2\text{CoO}_3]_{0.62}^{\text{RS}}[\text{CoO}_2]$  samples. Doping with Y and Bi increase  $T_{\text{SDW}}$  by  $\sim 40$  K and Sr-doping by  $\sim 20$  K, although Sr-doping did not affect  $T_{\text{SDW}}^{\text{on}}$  by the previous wTF- $\mu^+$ SR experiment.[13]

It should be noted that all the samples show approximately the same precession frequency ( $\sim 60$  MHz) at zero temperature. This suggests that the local magnetic field  $H_{\text{int}}(0 \text{ K})$  is independent of dopant. Since  $H_{\text{int}}$  in the doped  $[\text{Ca}_2\text{CoO}_3]$  subsystem should be strongly affected by the dopant, it is concluded that the IC-SDW exists not in the  $[\text{Ca}_2\text{CoO}_3]$  subsystem but in the  $[\text{CoO}_2]$  subsystem. Also, the latest  $\mu^+$ SR experiment on

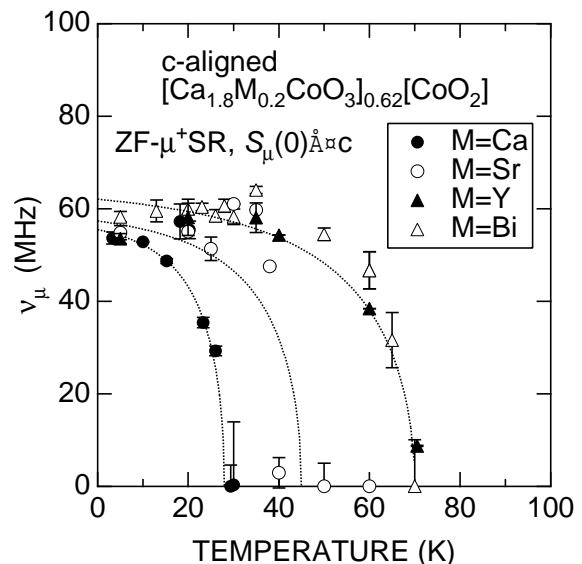


FIG. 4: Temperature dependences of  $\nu_{\mu}$  for the  $c$ -aligned pure and doped  $[\text{Ca}_2\text{CoO}_3]_{0.62}^{\text{RS}}[\text{CoO}_2]$ . The dotted lines represent the temperature dependence of the BCS gap energy.

$[\text{Ca}_2\text{Co}_{4/3}\text{Cu}_{2/3}\text{O}_4]_{0.62}[\text{CoO}_2]$ , [25] which consists of the quadruple rocksalt-type subsystem and the single  $[\text{CoO}_2]$  subsystem, also indicates the existence of an IC-SDW state below  $\sim 200$  K. The precession frequency due to an internal IC-SDW field is estimated as  $\sim 60$  MHz at zero temperature. This strongly suggests that the IC-SDW exists in the  $[\text{CoO}_2]$  subsystem, because one third of the Co ions in the rocksalt-type subsystem are replaced by Cu ions. Therefore, the IC-SDW is found to be caused by the spin-order of the conduction electrons in the  $[\text{CoO}_2]$  subsystem.

## B. Spin State Transition

The high-temperature wTF- $\mu^+$ SR spectra were measured in an air flow to avoid the formation of oxygen deficiency in the sample, whereas the previous experiment in vacuum. [14] The spectra in the  $c$ -aligned  $[\text{Ca}_2\text{CoO}_3]_{0.62}[\text{CoO}_2]$  sample were well fitted using an exponential relaxed cosine oscillation,  $A_{\text{PARA}} \exp(-\lambda_{\text{PARA}}t) \cos(\omega_{\mu}t + \phi)$ . Figures 5(a) - 5(d) show the temperature dependences of  $A_{\text{PARA}}$ ,  $\lambda_{\text{PARA}}$ , the shift of  $\omega_{\mu}$  ( $\Delta\omega_{\mu}$ ) and the inverse susceptibility  $\chi^{-1}$  in the  $c$ -aligned polycrystalline  $[\text{Ca}_2\text{CoO}_3]_{0.62}[\text{CoO}_2]$  sample and a polycrystalline  $[\text{Ca}_{1.8}\text{Y}_{0.2}\text{CoO}_3]_{0.62}[\text{CoO}_2]$  sample. Here,  $\Delta\omega_{\mu}$  is defined as  $(\omega_{\mu}(T) - \omega_{\mu}(300 \text{ K})) / \omega_{\mu}(300 \text{ K})$ ; since the oscillation of a reference was not measured,  $\Delta\omega_{\mu}$  is inequivalent to the muonic Knight shift.

A broad shoulder is clearly seen in the  $\lambda_{\text{PARA}}(T)$  curve of the pure sample at 400 - 600 K, although such a

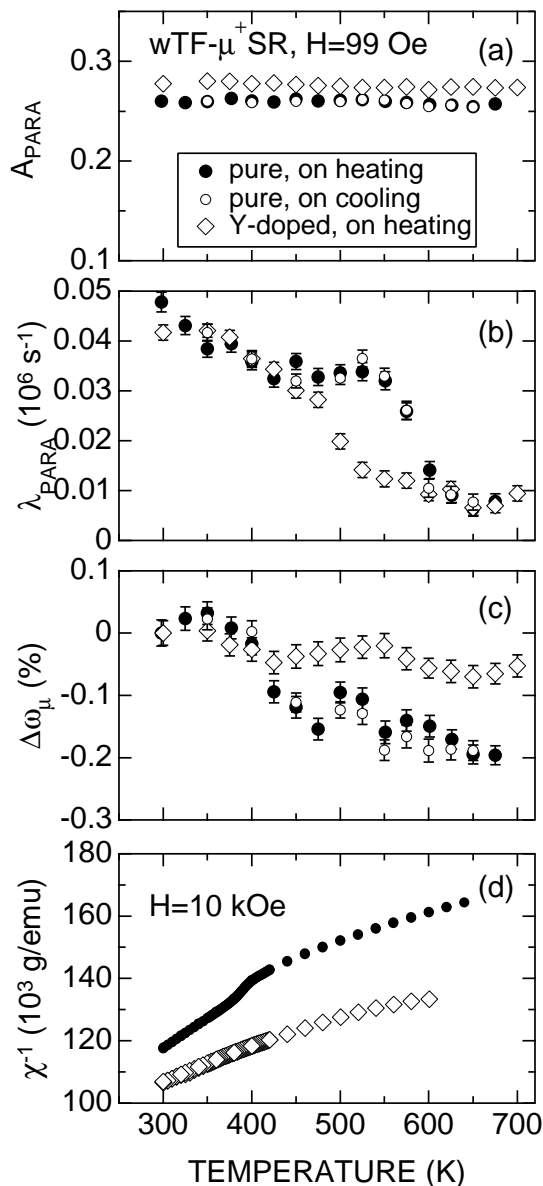


FIG. 5: Temperature dependences of (a) the asymmetry  $A_{\text{PARA}}$  (b) the muon spin relaxation rate  $\lambda_{\text{PARA}}$  (c) the shift of the muon precession frequency  $\Delta\omega_{\mu}$  and (d) the inverse susceptibility  $\chi^{-1}$  in a  $c$ -aligned polycrystalline  $[\text{Ca}_2\text{CoO}_3]_{0.62}[\text{CoO}_2]$  sample (circles) and a polycrystalline  $[\text{Ca}_{1.8}\text{Y}_{0.2}\text{CoO}_3]_{0.62}[\text{CoO}_2]$  sample (diamonds);  $A_{\text{PARA}}$  and  $\lambda_{\text{PARA}}$  was obtained by fitting the wTF- $\mu^+$ SR spectrum in the time domain using a simple exponential relaxation function,  $A_{\text{PARA}} \exp(-\lambda_{\text{PARA}}t) \cos(\omega_{\mu}t + \phi)$ .

shoulder seems to be ambiguous in the Y-doped sample [Fig. 5(b)]. Moreover, as  $T$  increases, the  $\Delta\omega_{\mu}(T)$  curve exhibits a sudden decrease at  $\sim 400$  K, while the  $\Delta\omega_{\mu}(T)$  curve in the Y-doped sample is roughly independent of  $T$ . It should be noted that, as seen in Figs. 1(a) and 5(a), above 150 K  $A_{\text{PARA}}$  levels off to its maximum

value ( $\sim 0.26$ ) — *i.e.* the sample volume is almost 100% paramagnetic. In addition, there is no thermal hysteresis in the data for the  $c$ -aligned  $[\text{Ca}_2\text{CoO}_3]_{0.62}[\text{CoO}_2]$  sample obtained on heating and on cooling. This suggests that the changes in the  $\lambda_{\text{PARA}}$  and the  $\Delta\omega_{\mu}$  are not caused by the formation of oxygen deficiency but by a magnetic transition, as discussed later.

These behaviors are in good agreement with the results of  $\chi(T)$  measurements. That is, the  $\chi^{-1}(T)$  curve of the pure sample exhibits an obvious change in slope at  $T_{\text{SS}}^{\chi} = 380$  K, while that of the Y-doped sample does not [Fig. 5(d)]. The change in the  $\chi^{-1}(T)$  curve is considered to be attributed to the spin state transition of the  $\text{Co}^{3+}$  and  $\text{Co}^{4+}$  ions from the low temperature  $LS$  or  $LS+IS$  to the high-temperature  $LS+IS$ ,  $IS$ ,  $IS+HS$  or  $HS$ , [2, 23] as in the case of  $\text{LaCoO}_3$ . [26, 27] Here  $LS$ ,  $IS$  and  $HS$  are the low-spin ( $t_{2g}^6$ ;  $S=0$  and  $t_{2g}^5$ ;  $S=1/2$ ), intermediate-spin ( $t_{2g}^5 e_g^1$ ;  $S=1$  and  $t_{2g}^4 e_g^1$ ;  $S=3/2$ ) and high-spin ( $t_{2g}^4 e_g^2$ ;  $S=2$  and  $t_{2g}^3 e_g^2$ ;  $S=5/2$ ) states, respectively.

At these temperatures muons are diffusing rapidly, so that the relaxation rate usually decreases monotonically with increasing temperature. Hence we can conclude that both the shoulder in the  $\lambda_{\text{PARA}}(T)$  curve and the sudden decrease in the  $\Delta\omega_{\mu}(T)$  curve are induced by the spin state transition, because there is no indications for the appearance of a magnetically ordered state (see Fig. 5(a)). Therefore, the spin state transition from the low-temperature  $LS$  to the high-temperature  $IS+HS$  or  $HS$  is most reasonable to explain the change in  $H_{\text{int}}$  (suggested by the changes in  $\lambda_{\text{PARA}}(T)$  and  $\Delta\omega_{\mu}(T)$ ) without the magnetic order, *i.e.*, the temperature independent  $A_{\text{PARA}}(T)$ . On the other hand, both the rapid muon diffusion and the fast exchange rate of electrons between  $\text{Co}^{3+}$  and  $\text{Co}^{4+}$  ions decrease  $\lambda_{\text{PARA}}$  with increasing  $T$ . The competition between these three factors is likely responsible for the broad shoulder in  $\lambda_{\text{PARA}}(T)$  around 400 - 600 K.

In order to know the contribution from the latter two factors, Fig. 6 shows the relationship between  $\lambda_{\text{PARA}}$  and  $T^{-1}$  of the pure and Y-doped samples, because the latter two factors are expected to depend on  $\exp(T^{-1})$ . Nevertheless, the linear relationship is not observed even in the Y-doped sample; thus, it is difficult to separate the contribution from each factor at present, although the difference between both samples are clearly seen in Fig. 6. Indeed, the  $\lambda_{\text{PARA}}(T)$  curves of the pure and Y-doped samples seem to level off to a constant value ( $\sim 0.01 \times 10^6 \text{ sec}^{-1}$ ) above 650 K due to a rapid muon diffusion, as in the case of  $\text{YBa}_2\text{Cu}_3\text{O}_{6\pm\delta}$ . [28, 29] Therefore, we can not determine the onset temperature ( $T_{\text{SS}}^{\text{on}}$ ) of the broad shoulder in the  $\lambda_{\text{PARA}}(T)$  curve, based only on the present  $\mu^+$ SR result, although  $T_{\text{SS}}^{\text{on}} \geq 600$  K. The broad shoulder also suggests the possibility that the spin state changes gradually above 400 K. In other words,  $T_{\text{SS}}^{\text{on}} \geq 600$  K and the endpoint  $T_{\text{SS}}^{\text{end}} = T_{\text{SS}}^{\chi} = 380$  K. And at temperatures between  $T_{\text{SS}}^{\text{on}}$  and  $T_{\text{SS}}^{\text{end}}$ , the populations

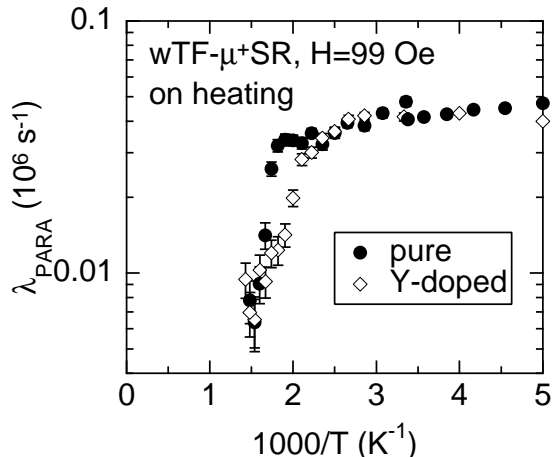


FIG. 6: Muon spin relaxation rate  $\lambda_{\text{PARA}}$  as a function of  $T^{-1}$  in a  $c$ -aligned polycrystalline  $[\text{Ca}_2\text{CoO}_3]_{0.62}^{\text{RS}}[\text{CoO}_2]$  sample (circles) and a polycrystalline  $[\text{Ca}_{1.8}\text{Y}_{0.2}\text{CoO}_3]_{0.62}[\text{CoO}_2]$  sample (diamonds). A discontinuity in data at 300 K was caused by the change in the experimental setup from a cryostat to an oven.

of the  $IS$  and  $HS$  states are likely to vary as a function of temperature, as in the case of  $\text{LaCoO}_3$ . [26, 27] The relationship between the spin state transition and the transport properties is discussed later.

## IV. DISCUSSION

### A. The nature of IC-SDW

There are two Co sites in the  $[\text{Ca}_2\text{CoO}_3]_{0.62}^{\text{RS}}[\text{CoO}_2]$  lattice; thus, it is difficult to determine the Co valence in the  $[\text{CoO}_2]$  plane by a  $\chi$  measurement or a chemical titration technique, although both  $\text{Co}^{3+}$  and  $\text{Co}^{4+}$  ions are mainly in the  $LS$  state below  $T_{\text{SS}}^{\text{end}}$ , according to the photo-emission and x-ray absorption studies on the related cobaltites,  $[\text{Sr}_2\text{Bi}_{2-y}\text{Pb}_y\text{O}_4]_x[\text{CoO}_2]$  [30] and  $\chi$  measurements on several cobaltites. [2, 3, 7, 13, 31] If we assume that only  $\text{Co}^{3+}$  and  $\text{Co}^{4+}$  ions exist in  $[\text{Ca}_2\text{CoO}_3]_{0.62}^{\text{RS}}[\text{CoO}_2]$  the average valence of the Co ions in the  $[\text{CoO}_2]$  plane is calculated as +3.38. This value is similar to the nominal valence of Co ions in  $\text{Na}_{0.6}\text{CoO}_2$ . Hence, the Co spins with  $S = 1/2$  are considered to occupy 40% corners in the two dimensional triangular lattice to minimize an electric repulsion and a geometrical frustration in the IC-SDW state.

It is worth noting that the  $\mu^+$  sites are bound to the O ions in the  $[\text{CoO}_2]$  plane. This means that the  $\mu^+$  mainly feel the magnetic field in the  $[\text{CoO}_2]$  plane. Thus, the IC-SDW is most unlikely to be caused by the misfit between the two subsystems, but to be an intrinsic be-

havior of the  $[\text{CoO}_2]$  plane. Nevertheless, the structure of the IC-SDW order is still unknown at present, because the current  $\mu^+$ SR experiments provide no information on the incommensurate wave vector. In order to obtain such information, it is necessary to carry out both  $^{59}\text{Co}$ -NMR and neutron scattering experiments on these cobaltites.

### B. Calculation and other experiments on IC-SDW

The IC-SDW order in  $[\text{Ca}_2\text{CoO}_3]_{0.62}^{\text{RS}}[\text{CoO}_2]$  is assigned to be a spin ( $S=1/2$ ) order on the two-dimensional triangular lattice at non-half filling. Such a problem was investigated by several workers using the Hubbard model within a mean field approximation; [32, 33, 34, 35]

$$H = -t \sum_{\langle ij \rangle \sigma} c_{i\sigma}^\dagger c_{j\sigma} + U \sum_i n_{i\uparrow} n_{i\downarrow}, \quad (5)$$

where  $c_{i\sigma}^\dagger$  ( $c_{j\sigma}$ ) creates (destroys) an electron with spin  $\sigma$  on site  $i$ ,  $n_{i\sigma} = c_{i\sigma}^\dagger c_{i\sigma}$  is the number operator,  $t$  is the nearest-neighbor hopping amplitude and  $U$  is the Hubbard on-site repulsion. The electron filling  $n$  is defined as  $n = (1/2N) \sum_i n_i$ , where  $N$  is the total number of sites. At  $T=0$  and  $n=0.5$  (i.e., the average valence of the Co ions in the  $[\text{CoO}_2]$  plane is +4), as  $U$  increased from 0, the system is paramagnetic metal up to  $U/t \sim 3.97$ , and changes into a metal with a spiral IC-SDW, and then at  $U/t \sim 5.27$ , a first-order metal-insulator transition occurs. [32] On the other hand, at  $n=0.81$  (i.e., the average valence of the Co ions in the  $[\text{CoO}_2]$  plane is +3.38), a spiral SDW state is stable below  $U/t \sim 3$ . [33] These calculations suggest that the IC-SDW state is stable for a weak-to-moderate coupling ( $U/t \leq 5$ ). Also, the IC-SDW phase boundary was reported to depend on  $n$ ; that is, in the  $n$  range between 0.75 and 1, the largest  $U/t$  for the IC-SDW phase increased monotonically with increasing  $n$ . [33] Since larger  $U/t$  stabilize the energy gap at higher temperature, [35] the calculations are consistent with the present  $\mu^+$ SR results, i.e., the large increase in  $T_{\text{SDW}}$  due to the Y- or Bi-doping into  $[\text{Ca}_2\text{CoO}_3]_{0.62}^{\text{RS}}[\text{CoO}_2]$ .

On the other hand, our preliminary heat capacity measurements using single crystal and  $c$ -aligned polycrystal  $[\text{Ca}_2\text{CoO}_3]_{0.62}^{\text{RS}}[\text{CoO}_2]$  samples indicate that the electronic specific heat parameter  $\gamma$  ranges from 60 to 90  $\text{mJ K}^{-2}$  per mol  $[\text{CoO}_2]$ , if we ignore the magnetic contribution. This value is higher than that for  $\text{Na}_x\text{CoO}_2$  with  $x \sim 0.5$  ( $\gamma \sim 24 \text{ mJ K}^{-2}$  per mol Co). [11] Thus,  $[\text{Ca}_2\text{CoO}_3]_{0.62}^{\text{RS}}[\text{CoO}_2]$  seems to be a strongly correlated electron system, as well as  $\text{Na}_x\text{CoO}_2$ . As a result, it is expected that  $U \gg t$ , although the above calculations suggest  $U/t \leq 5$ . In order to solve this puzzle, it is necessary to determine the IC-SDW structure at first.

According to the recent photoelectron spectroscopic study on  $[\text{Ca}_2\text{CoO}_3]_{0.62}^{\text{RS}}[\text{CoO}_2]$  below ambient temperature, the density of states DOS at the Fermi level  $E_{\text{F}}$  de-

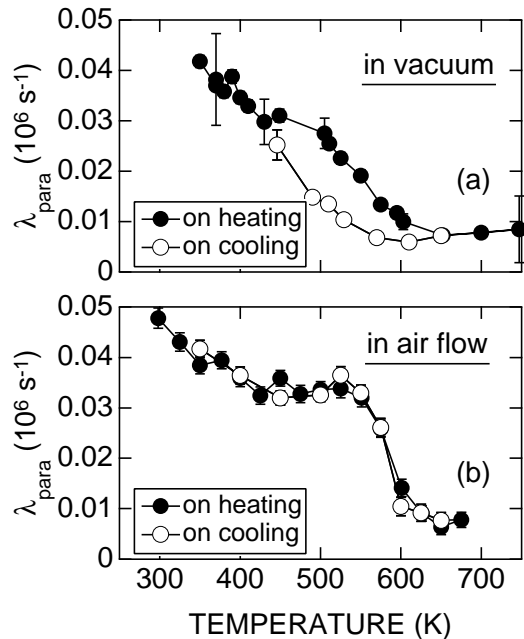


FIG. 7: Temperature dependences of the muon spin relaxation rate  $\lambda_{\text{para}}$  for the  $[\text{Ca}_2\text{CoO}_3]_{0.62}[\text{CoO}_2]$  sample measured (a) in vacuum[14] and (b) in an air flow.

creased with decreasing  $T$  and disappeared at 10 K.[36] Thus, the energy gap was clearly observed at 10 K. This also supports our conclusion; that is, both the broad minimum at  $\sim 80$  K in the  $\rho(T)$  curve and the rapid increase in  $\rho$  below 80 K with decreasing  $T$  are caused by the IC-SDW order between the spins of the conduction electrons and not by a magnetic scattering, such as, the Kondo effect.

### C. Effect of Oxygen Deficiency on Spin State Transition

In order to know the effect of atmosphere during the measurement, Fig. 7 shows the comparison of the previous[14] and the present  $\lambda_{\text{para}}(T)$  curve; the former was measured in vacuum and the latter in an air flow. There is a clear thermal hysteresis in the  $\lambda_{\text{para}}(T)$  curve obtained in vacuum. In addition, the broad maximum between 400 and 600 K looks very ambiguous in the data obtained in vacuum compared with that in an air flow. Recently, it was reported that oxygens are removed from  $[\text{Ca}_2\text{CoO}_3]_{0.62}[\text{CoO}_2]$  above 723 K (= 450 °C) even in an oxygen flow.[37] Therefore, both the clear thermal hysteresis and the suppression of the broad maximum in the  $\lambda_{\text{para}}(T)$  curve obtained in vacuum are induced by the formation of oxygen deficiency. As well as the oxygen deficiency, the substitution of Ca by Y decreases the average Co valence:[13] as a result, the  $\lambda_{\text{para}}(T)$  curve of the Y-doped sample looks quite similar to that of

$[\text{Ca}_2\text{CoO}_3]_{0.62}[\text{CoO}_2]$  obtained in vacuum on cooling (see Fig. 5(b) and Fig. 7(a)).

### D. Relationship between Spin State Transition and Transport Properties

The broad shoulder in the  $\lambda_{\text{para}}(T)$  curve at 400 - 600 K is in good agreement with the behavior of the  $\rho(T)$  curve, because the  $\rho(T)$  curve shows a broad maximum between 400 and 600 K, and above 600 K  $\rho$  decreases monotonically with increasing  $T$  up to 1000 K.[2, 38] On the other hand, the  $S(T)$  curve exhibits a small change in slope around  $T_{\text{SS}}^{\text{x}}$ ; that is, as  $T$  increases from 0 K,  $S$  increases monotonically up to  $\sim 100$  K and seems to level off a constant value ( $\sim 130 \mu\text{VK}^{-1}$ ) up to  $\sim 400$  K, then  $S$  again increases linearly ( $dS/dT \sim 80 \text{ nVK}^{-2}$ ) up to 1000 K.[2, 38] Therefore, above  $T_{\text{SS}}^{\text{end}}$ , the  $\rho(T)$  curve exhibits a semiconducting behavior, whereas the  $S(T)$  curve metallic.

The two Co sites in the  $[\text{Ca}_2\text{CoO}_3]_{0.62}^{\text{RS}}[\text{CoO}_2]$  lattice leads to a question which is responsible for the spin state transition, as in the case of IC-SDW order. Both the change in slope of  $S(T)$  at  $\sim 400$  K and the broad maximum of  $\rho(T)$  at 400 - 600 K suggest that the Co ions in the  $[\text{CoO}_2]$  plane play a significant role on the spin state transition. Indeed, the related cobaltites,  $\text{Na}_{0.9}[\text{CoO}_2]$  and  $\text{Na}_x\text{Ca}_y[\text{CoO}_2]$ , were reported to exhibit a small magnetic anomaly around 300 K, [46, 47] probably indicating the existence of a spin state transition, although the  $[\text{CoO}_2]$  plane was considered to be rigid due to a network of edge-sharing  $\text{CoO}_6$  octahedra. Hence, the Co ions in the  $[\text{CoO}_2]$  planes are most likely to change their spin state at 400 - 600 K.

The existence of the spin state transition suggests that the crystal-field splitting between  $t_{2g}$  and  $e_g$  levels is comparable to  $\sim 400$  K. Thus, above  $T_{\text{SS}}^{\text{end}}$ , charge carrier transport in the  $[\text{CoO}_2]$  plane is considered to be dominated by not only the direct hopping of the  $t_{2g}$  electrons between the Co ions [39] but also the hybridization between  $\text{Co-}e_g$  levels and  $\text{O-}2p$  levels, as in the case of the perovskite  $\text{LaCoO}_3$ . [40] Indeed,  $\rho$  of  $\text{LaCoO}_3$  decreased with increasing  $T$  above 500 K,[41] which is the temperature of the apparent spin state transition from  $LS$  to  $IS$  accompanied with an insulator-to-metal transition.

If we employ the modified Heikes formula using the degeneracy of spin and orbital degrees of freedom of Co ions,[42] the value of  $S_{T \rightarrow \infty}$  is calculated as  $154 \mu\text{VK}^{-1}$ , when the concentration of  $\text{Co}^{4+}$  is equivalent to that of  $\text{Co}^{3+}$  and both  $\text{Co}^{3+}$  and  $\text{Co}^{4+}$  are in the  $LS$  state. In order to explain the observed  $S(T)$  curve above  $T_{\text{SS}}^{\text{end}}$ , it is necessary to assume that  $\text{Co}^{3+}$  is in the  $LS$  state and  $\text{Co}^{4+}$  in the  $LS + IS$  state; under this assumption, we obtain  $S_{T \rightarrow \infty} = 293 \mu\text{VK}^{-1}$ , although such inequivalent spin state is unlikely to exist at elevated temperatures.

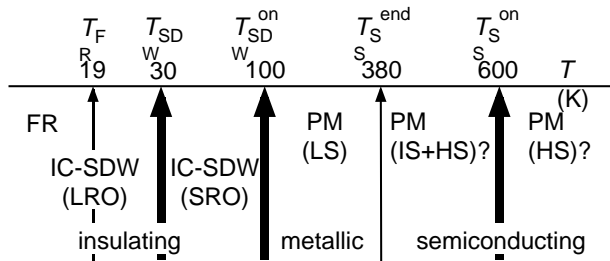


FIG. 8: Successive magnetic transitions in  $[\text{Ca}_2\text{CoO}_3]_{0.62}[\text{CoO}_2]$ . The bold arrows indicate the transitions found by the present and the previous  $\mu^+$ SR experiments, [13, 14] while the narrow arrows show those detected by the previous susceptibility measurements.[2, 13] In Fig. 8, FR means ferrimagnetic, PM paramagnetic and LS, IS and HS low-, intermediate- and high-spin state, respectively; and IC-SDW incommensurate spin density wave state, LRO and SRO long-range and short-range order. The spin states above  $T_{\text{SS}}^{\text{end}} \approx 380$  K are not clear at present.

Our  $\chi$  measurements using single crystal platelets of  $[\text{Ca}_2\text{CoO}_3]_{0.62}[\text{CoO}_2]$  showed a clear thermal hysteresis with a width of  $\sim 25$  K for the spin state transition at  $T_{\text{SS}}^{\text{end}}$ . [23] The thermal hysteresis was also confirmed by a heat capacity measurement.[43] These indicate that the spin state transition accompanies a structural change, as well as the case of  $\text{LaCoO}_3$  around 100 K and 500 K detected by neutron diffraction measurements. [44, 45]

Hence, in order to elucidate the mechanism of the spin state transition, further  $\mu^+$ SR experiments on the related cobaltites, such as  $\text{Na}_{0.9}[\text{CoO}_2]$  and  $\text{Na}_x\text{Ca}_y[\text{CoO}_2]$ , are necessary; in particular, a precise muonic Knight shift measurement would provide a significant information on the change in  $H_{\text{int}}$  during the spin state transition. In addition, we need an x-ray and/or neutron diffraction analysis for  $[\text{Ca}_2\text{CoO}_3]_{0.62}^{\text{RS}}[\text{CoO}_2]$  as a function of temperature, to obtain the information on structural change, which would affect the magnitude and distribution of  $H_{\text{int}}$  above  $T_{\text{SS}}^{\text{end}}$ . Furthermore, the photo-emission and x-ray absorption studies on  $[\text{Ca}_2\text{CoO}_3]_{0.62}[\text{CoO}_2]$  at elevated temperatures are needed to determine the spin state for understanding the transport properties above  $T_{\text{SS}}^{\text{end}}$ .

## V. SUMMARY

We investigated the magnetism of the misfit layered cobaltite,  $[\text{Ca}_2\text{CoO}_3]_{0.62}[\text{CoO}_2]$ , by a positive muon spin

rotation and relaxation experiment. It is found that  $[\text{Ca}_2\text{CoO}_3]_{0.62}[\text{CoO}_2]$  exhibits the successive magnetic transitions, as summarized in Fig. 8. An incommensurate (IC) spin density wave (SDW) is observed directly by ZF- $\mu^+$ SR below about 30 K, and evidence for the onset of the IC-SDW state is seen below  $T_{\text{SDW}}^{\text{on}} \approx 100$  K, while the muon spin relaxation is characteristic of a paramagnet (PM) above  $T_{\text{SDW}}^{\text{on}}$ . Therefore, we conclude that the long-range IC-SDW order completes below  $\sim 30$  K, whereas the short-range order appears below 100 K. Also the IC-SDW is found to propagate in the  $[\text{CoO}_2]$  plane, with oscillating moments directed along the  $c$ -axis. Below  $T_{\text{FR}} \approx 19$  K, the IC-SDW apparently coexists with ferrimagnetism (FR).

At 400 - 600 K, the spin state of Co ions changes; that is, the populations of the low-, intermediate- and high-spin states are most likely to vary gradually with increasing temperature above 380 K ( $= T_{\text{SS}}^{\text{end}}$ ). Also, this transition is found to be sensitive to the Co valence, which is controlled by doping and/or oxygen deficiency.

These two magnetic transitions detected by  $\mu^+$ SR are found to correlate closely with the transport properties of  $[\text{Ca}_2\text{CoO}_3]_{0.62}[\text{CoO}_2]$ ; in particular, both a broad minimum at around 80 K and a broad maximum between 400 and 600 K in the  $\rho(T)$  curve.

## Acknowledgments

We thank Dr. S.R. Kreitzman, Dr. B. Hitti and Dr. D.J. Arseneau of TRIUMF for help with the  $\mu^+$ SR experiments. Also, we thank Mr. A. Izadi-Najafabadi and Mr. S.D. LaRoy of University of British Columbia for help with the experiments. We appreciate useful discussions with Dr. R. Asahi of Toyota Central R&D Labs., Inc., Prof. U. Mizutani, Prof. H. Ikuta and Prof. T. Takeuchi of Nagoya University and Prof. K. Machida of Okayama University. This work was supported at Toyota CRDL by joint research and development with International Center for Environmental Technology Transfer in 2002-2004, commissioned by the Ministry of Economy Trade and Industry of Japan, at UBC by the Canadian Institute for Advanced Research, the Natural Sciences and Engineering Research Council of Canada, and at TRIUMF by the National Research Council of Canada.

[1] R. Funahashi, I. Matsubara, H. Ikuta, T. Takeuchi, U. Mizutani, and S. Sodeoka; *Jpn. J. Appl. Phys.* **39**, L1127



- [2] A. C. Masset, C. Michel, A. Maignan, M. Hervieu, O. Toulemonde, F. Studer, B. Raveau, and J. Hejtmanek; *Phys. Rev. B* **62**, 166 (2000).
- [3] Y. Miyazaki, K. Kudo, M. Akoshima, Y. Ono, Y. Koike, and T. Kajitani; *Jpn. J. Appl. Phys.* **39**, L531 (2000).
- [4] J. Molenda, C. Delmas, P. Dordor, and A. Stoklosa, *Solid State Ionics*, **12**, 473 (1989).
- [5] H. Yakabe, K. Kikuchi, I. Terasaki, Y. Sasago, K. Uchinokura, in *Proc. 16th Int. Conf. Thermoelectrics*, Dresden, 1997 (Institute of Electrical and Electronics Engineers, Piscataway, 1997), pp.523-527.
- [6] I. Terasaki, Y. Sasago, and K. Uchinokura, *Phys. Rev. B* **56**, R12685 (1997).
- [7] I. Tsukada, T. Yamamoto, M. Takagi, T. Tsubone, S. Konno, and K. Uchinokura, *J. Phys. Soc. Jpn.* **70**, 834 (2001).
- [8] T. Yamamoto, K. Uchinokura, and I. Tsukada, *Phys. Rev. B* **65**, 184434 (2002).
- [9] T. Fujii, I. Terasaki, T. Watanabe, and A. Matsuda, *Jpn. J. Appl. Phys.* **41**, L783 (2002).
- [10] Y. Miyazaki, T. Miura, Y. Ono, and T. Kajitani, *Jpn. J. Appl. Phys.* **41**, L849 (2002).
- [11] Y. Ando, N. Miyamoto, K. Segawa, T. Kawata, and I. Terasaki, *Phys. Rev. B* **60**, 10580 (1999).
- [12] Y. Miyazaki, M. Onoda, T. Oku, M. Kikuchi, Y. Ishii, Y. Ono, Y. Morii, and T. Kajitani; *J. Phys. Soc. Jpn.* **71**, 491 (2002).
- [13] J. Sugiyama, H. Itahara, T. Tani, J. H. Brewer, and E. J. Ansaldo, *Phys. Rev. B* **66**, 134413 (2002).
- [14] J. Sugiyama, J. H. Brewer, E. J. Ansaldo, M. Bayer, H. Itahara, and T. Tani, *Physica B* **326**, 518 (2003).
- [15] T. Tani, *J. Kore. Phys. Soc.* **32**, S1217 (1998).
- [16] M. Shikano, and R. Funahashi, in *Proc. 21st Int. Conf. Thermoelectrics*, Long Beach, 2002 (Institute of Electrical and Electronics Engineers, Piscataway, 2002), pp.192-194
- [17] T. Tani, H. Itahara, C. Xia, and J. Sugiyama, *J. Mat. Chem.* (2003) (in press).
- [18] C. Xia, J. Sugiyama, H. Itahara, and T. Tani, (unpublished).
- [19] L. P. Le, A. Keren, G. M. Luke, B. J. Sternlieb, W. D. Wu, Y. J. Uemura, J. H. Brewer, T. M. Riseman, R. V. Upasani, L. Y. Chiang, W. Kang, P. M. Chaikin, T. Csiba, and G. Grüner; *Phys. Rev. B* **48**, 7284 (1993).
- [20] Y. J. Uemura, in *Muon Science* edited by S. L. Lee et al., (Institute of Physics Publishing, Bristol, 1999) pp. 85-114, and references cited therein.
- [21] G. M. Kalvius, D. R. Noakes, and O. Hartmann, in *Handbook on the Physics and Chemistry of Rare Earths* **32** edited by K. A. Gschneidner Jr. et al., (North-Holland, Amsterdam, 2001) pp. 55-451, and references cited therein.
- [22] K. M. Kojima, Y. Fudamoto, M. Larkin, G. M. Luke, J. Merrin, B. Nachumi, Y. J. Uemura, M. Hase, Y. Sasago, K. Uchinokura, Y. Ajiro, A. Revcolevschi, and J. -P. Renard, *Phys. Rev. Lett.* **79**, 503 (1997).
- [23] J. Sugiyama, C. Xia, and T. Tani, *Phys. Rev. B* **67**, 104410 (2003).
- [24] G. Grüner; *Density Waves in Solids* Chap. 4 (Addison-Wesley-Longmans, Reading, 1994), and references cited therein.
- [25] J. Sugiyama, J. H. Brewer, E. J. Ansaldo, H. Itahara, K. Dohmae, C. Xia, and T. Tani, (unpublished).
- [26] J. B. Goodenough, *Magnetism and the chemical bond* (Wiley, New York, 1963), and references cited therein.
- [27] T. Saitoh, T. Mizokawa, A. Fujimori, M. Abbate, Y. Takeda, and M. Takano, *Phys. Rev. B* **55**, 4257 (1997).
- [28] J. H. Brewer, E. J. Ansaldo, J. F. Carolan, A. C. D. Chaklader, W. N. Hardy, D. R. Harshman, M. E. Hayden, M. Ishikawa, N. Kaplan, R. Keitel, J. Kempton, R. F. Kiefl, W. J. Kossler, S. R. Kreitzman, A. Kulpa, Y. Kuno, G. M. Luke, H. Miyatake, K. Nagamine, Y. Nakazawa, N. Nishida, K. Nishiyama, S. Ohkuma, T. M. Riseman, G. Roehmer, P. Schleger, D. Shimada, C. E. Stronach, T. Takabatake, Y. J. Uemura, Y. Watanabe, D. Ll. Williams, T. Yamazaki, and B. Yang, *Phys. Rev. Lett.* **60**, 1073 (1988).
- [29] J. H. Brewer, J. F. Carolan, W. N. Hardy, H. Hart, R. Kadono, J. R. Kempton, R. F. Kiefl, S. R. Kreitzman, G. M. Luke, T. M. Riseman, P. Schleger, B. J. Sternlieb, Y. J. Uemura, D. Ll. Williams and B. X. Yang, *Physica C* **162-164**, 157-158 (1989).
- [30] T. Mizokawa, L. H. Tjeng, P. G. Steeneken, N. B. Brookes, I. Tsukada, T. Yamamoto, and K. Uchinokura, *Phys. Rev. B* **64**, 115104 (2001).
- [31] R. Ray, A. Ghoshray, K. Ghoshray, and S. Nakamura, *Phys. Rev. B* **59**, 9454 (1999).
- [32] H. R. Krishnamurthy, C. Jayaprakash, S. Sarker, and W. Wenzel, *Phys. Rev. Lett.* **64**, 950 (1990).
- [33] M. Fujita, M. Ichimura, and K. Nakao, *J. Phys. Soc. Jpn.* **60**, 2831 (1991).
- [34] M. Fujita, T. Nakanishi, and K. Machida, *Phys. Rev. B* **45**, 2190 (1992).
- [35] M. C. Refolio, J. M. López Sancho, and J. Rubio, *Phys. Rev. B* **65**, 075114 (2002).
- [36] T. Takeuchi, K. Soda, H. Ikuta, U. Mizutani, M. Shikano, and R. Funahashi, in *Meeting Abstracts of Phys. Soc. Jpn.* **58** 523 (The Physical Society of Japan, Tokyo, 2003) in Japanese.
- [37] J. Shimoyama, K. Otzsch, M. Suzuki, S. Horii, and K. Kishio, in *Extended Abstracts of 48th Autumn Meeting of Jpn. Soc. Appl. Phys.* 128 (The Japan Society of Applied Physics, Tokyo, 2001) in Japanese.
- [38] Y. Miyazaki, T. Miura, Y. Ono, T. Akashi, T. Goto, and T. Kajitani, in *Proc. 21st Int. Conf. Thermoelectrics*, Long Beach, 2002 (Institute of Electrical and Electronics Engineers, Piscataway, 2002), pp.226-229.
- [39] D. J. Singh, *Phys. Rev. B* **61**, 13397 (2000).
- [40] M. A. Korotin, S. Yu. Ezhov, I. V. Solov'yev, and V. I. Anisimov, D. I. Khomskii, and G. A. Sawatzky, *Phys. Rev. B* **54**, 5309 (1996).
- [41] S. R. English, J. Wu, and C. Leighton, *Phys. Rev. B* **65**, 220407 (2002).
- [42] W. Koshibae, K. Tsutsui, and S. Maekawa, *Phys. Rev. B* **62**, 6869 (2000).
- [43] R. Asahi, (private communication).
- [44] K. Asai, O. Yokokura, N. Nishimori, H. Chou, J. M. Tranquada, G. Shirane, S. Higuchi, Y. Okajima and K. Kohn, *Phys. Rev. B* **50**, 3025 (1994).
- [45] K. Asai, A. Yoneda, O. Yokokura, J. M. Tranquada, G. Shirane, S. Higuchi, Y. Okajima and K. Kohn, *J. Phys. Soc. Jpn.* **67**, 290 (1998).
- [46] M. Mikami, Ph. D. thesis, Osaka University (2003) in Japanese; M. Mikami, M. Yoshimura, Y. Mori, T. Sasaki, R. Funahashi, and M. Shikano, (unpublished).
- [47] Y. Ono, M. Kato, Y. Miyazaki, and T. Kajitani, in *Extended Abstracts of 50th Spring Meeting of Jpn. Soc. Appl. Phys.* 245 (The Japan Society of Applied Physics, Tokyo, 2001) in Japanese.